

ratio, the pattern of spectra changed drastically, and a very sharp and intense band appeared at  $1985\text{ cm}^{-1}$ , (f). The observed i.r. spectra resembled those on supported Fe in CO chemisorption at  $35\text{ }^\circ\text{C}$ .<sup>5</sup> Eventually, the bands due to CO chemisorption on Pd were diminished in their intensities, (h).

As revealed by the appearance of the band at  $2015\text{ cm}^{-1}$  in (b), the reduced Fe metal was formed by a small addition of Fe to Pd, and this has been confirmed by the existence of  $\text{PdFe}^0$  bimetallic clusters revealed by Mössbauer spectroscopic studies.<sup>6,7</sup> It is, thus, speculated that the promotion of MeOH synthesis due to addition of Fe is associated with the creation of a special type of  $\text{PdFe}^0$  cluster, the concentration of which would depend upon the Fe content, giving a maximum promotion at around Fe/Pd 0.07. Indeed, the changes in the i.r. spectrum of CO absorption from (a) to (b) suggest that a modification of the surface site occurred on addition of a small amount of Fe (Fe/Pd  $<0.1$ ), and the number of special sites thus generated decreased with an increase of Fe content. It seems that the second modification in the morphology of the catalyst surface occurred at Fe/Pd 0.3, catalysing the formation of  $\text{CH}_4$ ,  $\text{C}_{2+}$  hydrocarbons, and  $\text{CO}_2$ , and this may correspond to the formation of the intermetallic compound  $\text{Pd}_3\text{Fe}$  in the phase diagram.<sup>8</sup> Here a spectral change was observed in Mössbauer spectra from a single peak, due to isolated  $\text{Fe}^0$ , to sextet peaks, due to the intermetallic compound.<sup>7</sup> The addition of an excess of Fe to Pd (Fe/Pd  $>0.3$ ) provided a phase of another intermetallic PdFe and a eutectic halt. The state of the newly developed eutectic phase remained almost constant in a range of Fe/Pd (0.3–0.5). The

phase was characteristic in producing  $\text{CO}_2$  and hydrocarbons in CO hydrogenation, as reflected in the decrease of total amounts of CO adsorbed on the catalyst surface (i.r. studies). Above Fe/Pd 0.5, the Pd surface may be covered with Fe, catalysing the typical Fischer–Tropsch synthesis to provide hydrocarbon from  $\text{CO} + \text{H}_2$ , as in the case of pure Fe/ $\text{SiO}_2$ .

This work is a part of 'C<sub>1</sub>-Chemistry project,' a National Research and Development Program of Agency of Industrial Science and Technology, Ministry of International Trade and Industry (M.I.T.I.), Japan.

Received, 2nd September 1985; Com. 1289

## References

- 1 M. L. Poutma, L. F. Elek, P. A. Risch, and J. A. Rabo, *J. Catal.*, 1978, **52**, 157.
- 2 M. M. Bhasin, W. J. Bartley, P. C. Ellegen, and T. P. Wilson, *J. Catal.*, 1978, **54**, 120.
- 3 T. Fukushima, Y. Ishii, Y. Onda, and M. Ichikawa, *J. Chem. Soc., Chem. Commun.*, 1985, 1752.
- 4 M. Ichikawa, T. Fukushima, and T. Shikakura, *Proc. Int. Congr. Pure Appl. Chem.*, 1984, **2**, 69.
- 5 R. P. Eischens and W. A. Pliskin, *Adv. Catal.*, 1958, **10**, 1.
- 6 R. L. Garten, *J. Catal.*, 1976, **43**, 18.
- 7 Y. Minai, T. Fukushima, M. Ichikawa, S. Ogasawara, and T. Tominaga, *J. Chem. Soc., Chem. Commun.*, submitted for publication.
- 8 O. Fubaschekovski, 'Iron-Binary Phase Diagram,' Springer-Verlag, Berlin, 1982.

## Novel C–C and C–N Coupling Reactions on a Di-iron- $\alpha$ -Di-imine Complex in the Reaction of $\text{Fe}_2(\text{CO})_6\{\text{RN}=\text{C}(\text{H})\text{C}(\text{H})=\text{NR}\}$ with Methyl Propynoate; X-Ray Crystal Structures of $\text{Fe}_2(\text{CO})_5\{\text{(c-C}_6\text{H}_{11})\text{N}=\text{CHCHN}(\text{c-C}_6\text{H}_{11})\text{C}(\text{O})\text{CH}=\text{CCO}_2\text{Me}\}$ , $\text{Fe}_2(\text{CO})_6\{\text{PriNCHCH}=\text{N}(\text{Pri})\text{CHCCO}_2\text{Me}\}$ and $\text{Fe}_2(\text{CO})_4\{\text{PriNCHCHN}(\text{Pri})\text{CHCCO}_2\text{Me}\}$

Fred Muller,<sup>a</sup> Gerard van Koten,<sup>a</sup> Kees Vrieze,<sup>\*a</sup> Bert Krijnen,<sup>b</sup> and Casper H. Stam<sup>b</sup>

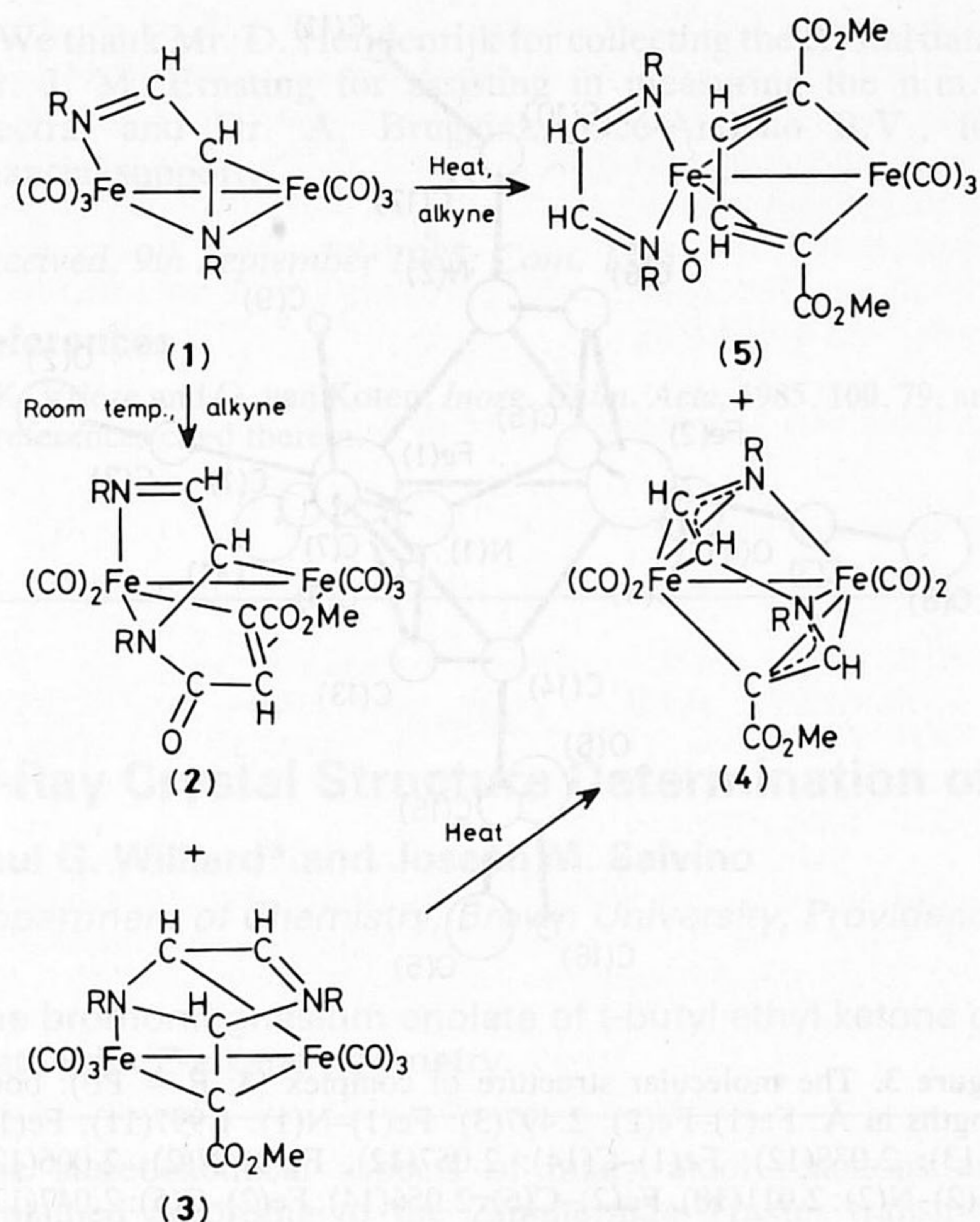
<sup>a</sup> *Laboratorium voor Anorganische Chemie, and* <sup>b</sup> *Laboratorium voor Kristallografie, University of Amsterdam, J. H. van't Hoff Instituut, Nieuwe Achtergracht 166, 1018 WV Amsterdam, The Netherlands*

The reaction of  $\text{Fe}_2(\text{CO})_6(\text{Rdab})$  [ $\text{Rdab} = \text{RN}=\text{CHCH}=\text{NR}$ ;  $\text{R} = \text{Pri}$  or  $\text{c-C}_6\text{H}_{11}$  (cyclohexyl)] with methyl propynoate at room temperature yields two products (X-ray):  $\text{Fe}_2(\text{CO})_5\{\text{RN}=\text{CHCHN}(\text{R})\text{C}(\text{O})\text{CH}=\text{CCO}_2\text{Me}\}$ , where the Rdab ligand, a CO, and an alkyne are coupled to form an 8e donating ligand, and  $\text{Fe}_2(\text{CO})_6\{\text{RNCHCH}=\text{N}(\text{R})\text{CHCCO}_2\text{Me}\}$ , containing a 6e donating heterocyclic ligand, formed by coupling of the terminal alkyne C atom to both the Rdab N atoms in an unusual fashion; heating of the latter complex yields  $\text{Fe}_2(\text{CO})_4\{\text{RNCHCHN}(\text{R})\text{CHCCO}_2\text{Me}\}$  (X-ray), with an unprecedented bis- $\eta^3$ -aza-allyl bonded ligand.

We have already shown that the  $\alpha$ -diimine ligand Rdab ( $\text{RN}=\text{CHCH}=\text{NR}$ ;  $\text{dab} = 1,4\text{-diazabuta-1,3-diene}$ ), when co-ordinated as a  $\sigma\text{-N}, \sigma\text{-N}', \eta^2\text{-C}=\text{N}$  6e donor to transition metal atoms, may be involved in coupling reactions with unsaturated organic molecules, either *via* the C atom or *via* the N atom of the  $\eta^2\text{-C}=\text{N}$  bonded part of the ligand. Examples of these reactions are those with Rdab itself, and with carbodiimines ( $\text{RN}=\text{C}=\text{NR}$ ), sulphines ( $\text{R}_2\text{C}=\text{S}=\text{O}$ ), alkynes, and ketene.<sup>1,2</sup> An interesting aspect of the reactions of  $\text{Ru}_2(\text{CO})_6(\text{Rdab})$  with mono- and di-substituted alkynes is the ability of this complex to act as a cyclotrimerisation catalyst. Especially interesting was the selective formation of 1,3,5-trisubstituted benzene derivatives, when monosubstituted

alkynes were used. Recently Frühauf *et al.* showed that mononuclear iron–Rdab complexes react under CO pressure with activated alkynes to give also C–C and C–N coupled products.<sup>3</sup> These and results for Ru-complexes stimulated us to study the reactivity of dinuclear  $\text{Fe}_2(\text{CO})_6(\text{Rdab})$  complexes towards alkynes.<sup>4</sup>

We now report results for the reactions of  $\text{Fe}_2(\text{CO})_6(\text{Rdab})$  complexes ( $\text{R}=\text{Pri}$  or  $\text{c-C}_6\text{H}_{11}$ ) (**1**) with methyl propynoate. Upon treating (**1**) with a threefold excess of  $\text{HC}\equiv\text{CCO}_2\text{Me}$  at room temperature a mixture of complexes (**2**) and (**3**) was formed, which could be separated by column chromatography on silica. Heating of the dark yellow complex (**3**) for 2 h at  $90\text{ }^\circ\text{C}$  afforded in almost quantitative yield the brown complex



**Scheme 1.** Reaction of  $\text{Fe}_2(\text{CO})_6(\text{Rdab})$  (1) [R = Pr<sup>i</sup> or *c*-C<sub>6</sub>H<sub>11</sub> (cyclohexyl)] with methyl propynoate (alkyne).

(4). This complex was also formed when (1) was heated with an excess of HC≡CCO<sub>2</sub>Me in heptane for about 24 h. In that case, however, the yield was low (<10%) and the main product was the intensely purple coloured complex (5).<sup>†</sup> These reactions are summarized in Scheme 1.<sup>‡</sup> The molecular structures of (2), (3) and (4) have been established by single-crystal X-ray diffraction.<sup>§</sup>

<sup>†</sup> In this complex the two alkyne atoms are tail-to-tail coupled and are  $\sigma, \sigma$ -bonded to one of the iron atoms to form a metallacyclopentadiene fragment. The latter fragment is  $\eta^2, \eta^2$ -co-ordinated to a second Fe atom, to which also the Rdab ligand is co-ordinated in the chelate bonding mode.

<sup>‡</sup> Important <sup>1</sup>H n.m.r. data (CDCl<sub>3</sub>; proton numbering corresponds to C atom numbering in Figures 1–3): (2; R = Pr<sup>i</sup>),  $\delta$  7.86 (12-H), 2.84 (11-H), <sup>3</sup>J<sub>11,12</sub> 2.2 Hz, and 4.21 (7-H); (3; R = Pr<sup>i</sup>),  $\delta$  6.71 (10-H), 3.75 (9-H), <sup>3</sup>J<sub>9,10</sub> 5.2 Hz, and 6.6 (8-H, br. owing to quadrupole relaxation due to the N atoms), <sup>4</sup>J<sub>8,9</sub> 1.1 Hz; (4; R = Pr<sup>i</sup>),  $\delta$  8.41 (13-H), 8.19 (5-H), and 7.73 (6-H), <sup>3</sup>J<sub>5,6</sub> 8, <sup>4</sup>J<sub>5,13</sub> 1.6 Hz.

<sup>§</sup> *Crystal Data* (all structures were solved by the heavy atom method; refinement using anisotropic block-diagonal least-squares calculations): (2) *M* = 584.19, monoclinic, space group *P*2<sub>1</sub>/*n*, *Z*(C<sub>24</sub>H<sub>28</sub>N<sub>2</sub>O<sub>8</sub>Fe<sub>2</sub>) = 4, *a* = 20.979(2), *b* = 8.9658(8), *c* = 14.693(1),  $\beta$  = 107.393(9)°,  $\mu(\text{Cu-K}\alpha)$  = 97.2 cm<sup>-1</sup>. H atoms were in calculated positions and not refined; *R* = 0.060, *R*<sub>w</sub> = 0.069 for 1034 absorption-corrected reflections. (3) *M* = 504.06, monoclinic, space group *P*2<sub>1</sub>/*n*, *Z*(C<sub>18</sub>H<sub>20</sub>N<sub>2</sub>O<sub>8</sub>Fe<sub>2</sub>) = 4, *a* = 12.757(1), *b* = 18.247(1), *c* = 9.662(3) Å,  $\beta$  = 107.35(1)°,  $\mu(\text{Mo-K}\alpha)$  = 14.61 cm<sup>-1</sup>, isotropic refinement for H, *R* = 0.045, *R*<sub>w</sub> = 0.085 for 3717 absorption-corrected reflections. (4) *M* = 448.04, orthorhombic, space group *Pnca*, *Z*(C<sub>16</sub>H<sub>20</sub>N<sub>2</sub>O<sub>6</sub>Fe<sub>2</sub>) = 4, *a* = 15.209(3), *b* = 17.685(3), *c* = 14.489(3) Å,  $\mu(\text{Mo-K}\alpha)$  = 7.60 cm<sup>-1</sup>, H-atoms were excluded, *R* = 0.076, *R*<sub>w</sub> = 0.142 for 1320 absorption-corrected reflections. The atomic co-ordinates for this work are available on request from the Director of the Cambridge Crystallographic Data Centre, University Chemistry Laboratory, Lensfield Road, Cambridge CB2 1EW. Any request should be accompanied by the full literature citation for this communication.

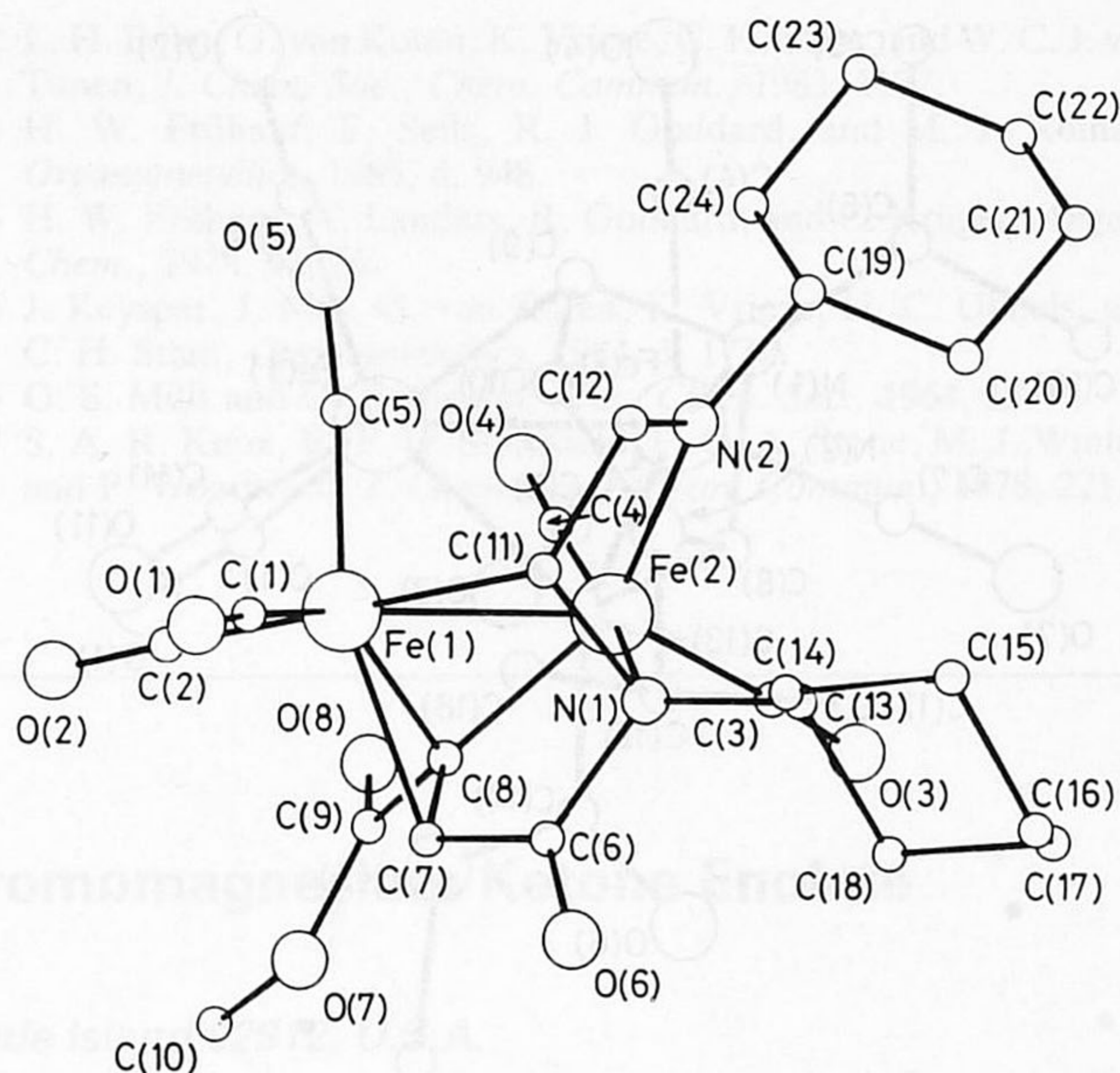


**Figure 1.** The molecular structure of complex (2; R = *c*-C<sub>6</sub>H<sub>11</sub>): bond lengths in Å: Fe(1)–Fe(2): 2.631(4), Fe(1)–C(8): 2.046(14), Fe(1)–C(7): 2.084(12), Fe(1)–C(11): 2.138(12), Fe(2)–C(8): 1.883(14), Fe(2)–N(1): 2.098(9), Fe(2)–N(2): 1.999(11), C(7)–C(8): 1.403(18), C(7)–C(6): 1.450(17), C(6)–O(6): 1.220(18), C(6)–N(1): 1.471(19), N(1)–C(11): 1.462(16), C(11)–C(12): 1.530(19), C(12)–N(2): 1.236(17).

The brown complex (2) consists of an Fe<sub>2</sub>(CO)<sub>5</sub> unit [Fe(1)–Fe(2): 2.631(4) Å] bridged by a 8e donating dianionic organic ligand. This ligand is formed by coupling of the Rdab ligand with a CO and a HC≡CCO<sub>2</sub>Me unit. The triple bond of the alkyne fragment is reduced to a double bond, owing to the coupling of C(7) with a CO molecule, while C(8) is bridging between the two Fe atoms. The double bond is also asymmetrically  $\eta^2$ -co-ordinated to one of the Fe atoms [C(7)–Fe(1): 2.084(12), C(8)–Fe(1): 2.046(14) Å], confirmed by the elongation of the C(7)–C(8) bond [1.403(18) Å]. The shortening of the bond lengths in the C(7)–C(6)–N(1)–C(11) part of the ligand indicates some delocalization of the negative charge over these three bonds [C(7)–C(6): 1.450(17); C(6)–N(1): 1.471(19); N(1)–C(11): 1.462(16) Å]. However, no delocalization occurs over the C(11)–C(12)–N(2) part of the original Rdab skeleton, as is clearly indicated by the C(11)–C(12) single bond length [1.530(19) Å] and the normal imine bond length [C(12)–N(2): 1.236(17) Å].

In complex (3) the Fe<sub>2</sub>(CO)<sub>6</sub> unit [Fe–Fe: 2.563(4) Å] is bridged by a formally 6e donating ligand. An unusual feature is that in this ligand one of the alkyne C atoms is coupled to both the N atoms of the Rdab ligand, thus forming a five-membered heterocyclic ring. The other alkyne C atom symmetrically bridges the two Fe atoms [Fe(1)–C(13): 2.001(14), Fe(2)–C(13): 2.009(10) Å]. As can be seen from the C(8)–C(13) bond length of 1.523(5) Å, this former alkyne bond is reduced to a single bond with a change in hybridization of C(8) from sp to sp<sup>3</sup>. The imine bond N(2)–C(10) in the heterocyclic ring is slightly elongated [1.310(17) Å], while the C(9)–C(10) bond [1.425(11) Å] is somewhat short for a single bond. This indicates that the C(9)–C(10)–N(2) part of the ring has some allylic nature. This part of the ligand is probably best described as containing a positive charge on N(2) and a negative charge delocalized over the N(2)–C(10) and C(9)–C(10) bonds. The atoms C(9), C(10), N(2), and C(8) are

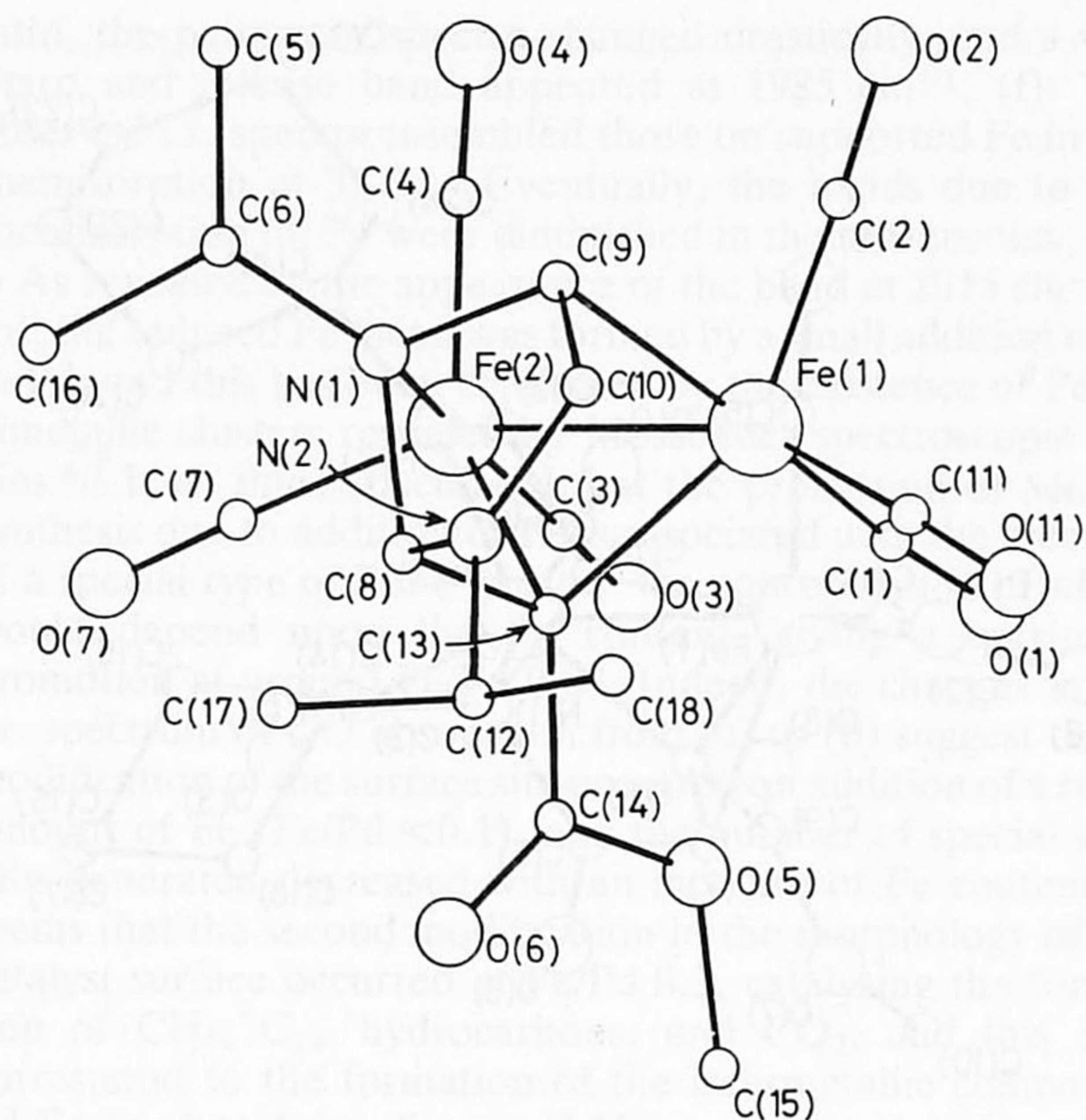


**Figure 2.** The molecular structure of complex (**3**; R = Pr<sup>i</sup>): bond lengths in Å: Fe(1)–Fe(2): 2.563(4), Fe(1)–C(9): 2.122(8), Fe(1)–C(13): 2.001(14), Fe(2)–N(1): 2.062(4), Fe(2)–C(13): 2.009(10), N(1)–C(9): 1.493(9), C(9)–C(10): 1.425(11), C(10)–N(2): 1.310(17), N(2)–C(8): 1.477(5), C(8)–N(1): 1.503(15), C(8)–C(13): 1.523(5).

coplanar (r.m.s. deviation 0.062 Å), while N(1) is 0.55 Å above this plane.

The framework of (**4**) consists of an Fe<sub>2</sub>(CO)<sub>4</sub> unit [Fe–Fe: 2.497(3) Å] with a 10e donating organic ligand bridging the two Fe atoms. This ligand can be seen as two coupled η<sup>3</sup>-bonded aza-allyl fragments, one of which consists of the N(2)–C(6)–C(5) part of the Rdab ligand and the other consisting of the originally bridging N atom, N(1), coupled with the terminal alkyne C atom, C(13), of the methyl propynoate. The η<sup>3</sup>-allylic nature of these two parts of the ligand is indicated by the bond lengths [Fe(2)–N(2): 2.011(10); Fe(2)–C(6): 2.056(14); Fe(2)–C(5): 2.047(12); N(2)–C(6): 1.380(19); C(6)–C(5): 1.459(21) Å] for the aza-allyl fragment bonded to Fe(2) and those [Fe(1)–N(1): 1.997(11); Fe(1)–C(13): 2.038(12); Fe(1)–C(14): 2.057(12); N(1)–C(13): 1.427(16); C(13)–C(14): 1.357(16) Å] for the aza-allyl fragment bonded to Fe(1). ¶ This complex shows some structural resemblance to the complexes Co<sub>2</sub>(CO)<sub>4</sub>{(Bu<sup>i</sup>C≡CH)<sub>2</sub>(HC≡CH)}<sup>6</sup> and Mo<sub>2</sub>(η<sup>5</sup>-C<sub>5</sub>H<sub>5</sub>)<sub>2</sub>{(PhC≡CH)<sub>2</sub>(HC≡CH)}<sup>7</sup> in which the three alkynes are coupled to form a ligand that co-ordinates *via* two η<sup>3</sup>-allyl functions to the Co<sub>2</sub>(CO)<sub>4</sub> and the Mo<sub>2</sub>(η<sup>5</sup>-C<sub>5</sub>H<sub>5</sub>)<sub>2</sub> unit respectively, while the two metal atoms are bridged by both the terminal C-atoms of the ligand skeleton.

The thermally induced rearrangement of (**3**) to (**4**) probably involves, besides the elimination of two CO ligands, the fission of the N(2)–C(8) bond, followed by rotation of the N(2)–C(9)–C(10) part of the ligand along the N(1)–C(9) bond. We cannot, however, exclude the possibility of cleavage of the N(1)–C(8) bond, which would afford the same end product.

¶ The distances in the aza-allyl fragments may be compared with similar bond lengths of 1.38(2) and 1.39(2) Å in MnFe(CO)<sub>6</sub>(Pr<sup>i</sup>NCHCHNPr<sup>i</sup>)<sup>5</sup> and 1.396(7) and 1.405(8) Å in Ru<sub>2</sub>(CO)<sub>5</sub>{Pr<sup>i</sup>NCHCHNPr<sup>i</sup>C(:O)CH<sub>2</sub>C(:O)CH<sub>2</sub>}<sup>2</sup>

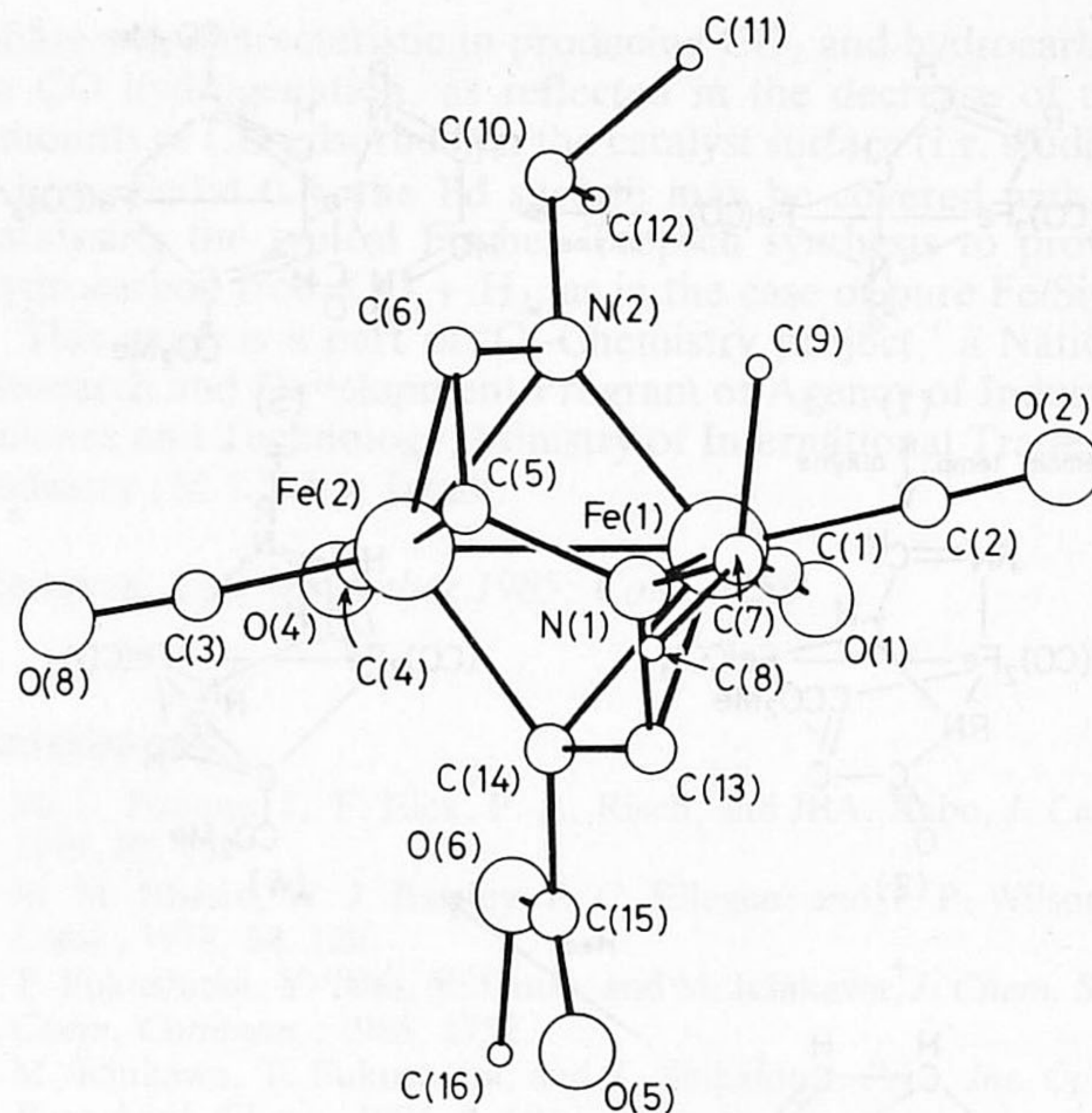


**Figure 3.** The molecular structure of complex (**4**; R = Pr<sup>i</sup>): bond lengths in Å: Fe(1)–Fe(2): 2.497(3); Fe(1)–N(1): 1.997(11), Fe(1)–C(13): 2.038(12), Fe(1)–C(14): 2.057(12), Fe(1)–N(2): 2.006(12), Fe(2)–N(2): 2.011(10), Fe(2)–C(6): 2.056(14), Fe(2)–C(5): 2.047(12), Fe(2)–C(14): 1.973(11), N(2)–C(6): 1.380(19), C(6)–C(5): 1.459(21), C(5)–N(1): 1.479(19), N(1)–C(13): 1.427(16), C(13)–C(14): 1.357(16). The terminal methyl C-atoms are drawn smaller for clarity.

Further delocalization of charge over the ligand then results in the formation of the bis-aza-allyl ligand in (**4**), which is the first example of its kind.

The present C–N and C–C coupling reactions take place with the dinuclear Fe<sub>2</sub>(CO)<sub>6</sub>(Rdab) complexes, which strongly suggests that the activation of η<sup>2</sup>-C=N part of the Rdab ligand as well as the electronic activation of the alkyne bond by the methoxycarbonyl group are important factors. The small steric hindrance of the methyl propynoate CH group seems likewise to be important as is indicated by the fact that the disubstituted analogue (MeO<sub>2</sub>CC≡CCO<sub>2</sub>Me) reacts with Fe<sub>2</sub>(CO)<sub>6</sub>(Rdab) in a quite different way.\*\* Other workers,<sup>3</sup> however, claim that η<sup>2</sup>-C=N co-ordination of the Rdab ligand is not necessary for the ligand to undergo C–N and C–C coupling reactions. This has been concluded from the observation that in the reaction of MeO<sub>2</sub>CC≡CCO<sub>2</sub>Me with the mononuclear complex Fe(CO)<sub>3</sub>(Rdab), where the ligand is 4e σ-N,σ-N'-chelate bonded to the Fe atom, complexes with complicated organic ligands resulting from C–C and C–N coupling reactions are also obtained. It must be noted, however, that the latter reaction only takes place under CO pressure, which makes it difficult to conclude that the Rdab ligand is σ-N,σ-N'-co-ordinated when the coupling reaction with the alkyne molecule takes place. We are currently studying further reactions of alkynes with dinuclear Fe complexes containing either 4e σ-N,σ-N'-co-ordinated or 6e σ-N,σ-N', η<sup>2</sup>-C=N-co-ordinated Rdab ligands.

\*\* In this reaction no coupling reaction with the Rdab ligand occurs, but one of the CO groups is substituted by an alkyne to form the complex Fe<sub>2</sub>(CO)<sub>5</sub>(Rdab)(alkyne). At 69 °C this reaction is followed by the substitution of a second CO group by an alkyne, which is then coupled to the first alkyne, to form an RCCRCRCR fragment co-ordinated to an Fe<sub>2</sub>(CO)<sub>4</sub> unit.

We thank Mr. D. Heijdenrijk for collecting the crystal data, Mr. J. M. Ernsting for assisting in measuring the n.m.r. spectra, and Dr. A. Bruggink, Océ-Andeno B.V., for financial support.

Received, 9th September 1985; Com. 1315

## References

1 K. Vrieze and G. van Koten, *Inorg. Chim. Acta*, 1985, **100**, 79, and references cited therein.

- 2 L. H. Polm, G. van Koten, K. Vrieze, C. H. Stam, and W. C. J. van Tunen, *J. Chem. Soc., Chem. Commun.*, 1983, 1177.  
 3 H. W. Frühauf, F. Seils, R. J. Goddard, and M. J. Romao, *Organometallics*, 1985, **4**, 948.  
 4 H. W. Frühauf, A. Landers, R. Goddard, and C. Krüger, *Angew. Chem.*, 1978, **90**, 56.  
 5 J. Keysper, J. Mul, G. van Koten, K. Vrieze, H. C. Ubbels, and C. H. Stam, *Organometallics*, 1984, **3**, 1732.  
 6 O. S. Mills and G. Robinson, *Proc. Chem. Soc.*, 1964, 187.  
 7 S. A. R. Knox, R. F. D. Stansfield, F. G. A. Stone, M. J. Winter, and P. Woodward, *J. Chem. Soc., Chem. Commun.*, 1978, 221.

## X-Ray Crystal Structure Determination of a Bromomagnesium Ketone Enolate

Paul G. Williard\* and Joseph M. Salvino

Department of Chemistry, Brown University, Providence, Rhode Island 02912, U.S.A.

The bromomagnesium enolate of t-butyl ethyl ketone crystallizes as a dimeric, ether solvated aggregate in the solid state with Z-alkene geometry.

The stereochemical aspects of many aldol reactions are explained according to the Zimmerman-Traxler transition state model.<sup>1</sup> The main feature of this model is metal-coordination-induced substrate organization. While the Zimmerman-Traxler ligated transition state model as applied to the aldol reaction remains extremely useful for predictive purposes, more recent studies on enolate alkylation by Jackman and others suggest that solution aggregation phenomena may complicate the simple Zimmerman-Traxler model.<sup>2</sup> The aldol reaction is especially susceptible to complications by aggregation phenomena because it is known to be fast and reversible.<sup>3</sup> Since aldol reaction products can be obtained either thermodynamically or kinetically, it is important to understand the aggregation state of the reactants and the steric requirements of the chelated aldolate ligands in order to predict and/or control aldol reaction stereochemistry. Hence, we initiated a crystallographic investigation to determine unambiguously the structure of a magnesium enolate, and also studied the role of this divalent metal cation in the aldol reaction. Herein we report the first X-ray crystal structure of a bromomagnesium ketone enolate.

The bromomagnesium enolate of t-butyl ethyl ketone was prepared by reduction of the  $\alpha$ -bromoketone (1) with Mg<sup>0</sup> in diethyl ether.<sup>4</sup> Concentration of this solution to > 1.0 M and cooling to -28 °C provided crystals suitable for X-ray diffraction analysis. The enolate (2) crystallizes as the solvated dimeric aggregate, (C<sub>7</sub>H<sub>13</sub>OMgBr)<sub>2</sub>·(C<sub>4</sub>H<sub>10</sub>O)<sub>2</sub>, and its structure is plotted in Figure 1.† This structure consists of a slightly puckered (Mg–O)<sub>2</sub> ring with bridging enolate oxygen atoms.

† Crystals of the solvated MgBr ketone enolate (2) are monoclinic, space group *P*2<sub>1</sub>/*c*, *a* = 10.217(5), *b* = 16.945(10), *c* = 17.282(11) Å,  $\beta$  = 98.26(5)°, *Z* = 4 (C<sub>7</sub>H<sub>13</sub>OMgBr)<sub>2</sub>·(C<sub>4</sub>H<sub>10</sub>O)<sub>2</sub> units, *D*<sub>c</sub> = 1.31 g/cm<sup>3</sup>. The final agreement factors are *R* = 0.0766 and *R*<sub>w</sub> = 0.0753 for 2520 unique observed [*F* ≥ 3σ(*F*)] reflections and 271 independent variables. We believe that the large thermal parameters for the terminal methyl carbon atom, C(18), of one of the solvating ethers represents disorder in the crystal. The atomic co-ordinates for this work are available on request from the Director of the Cambridge Crystallographic Data Centre, University Chemical Laboratory, Lensfield Rd., Cambridge CB2 1EW. Any request should be accompanied by the full literature citation for this communication.

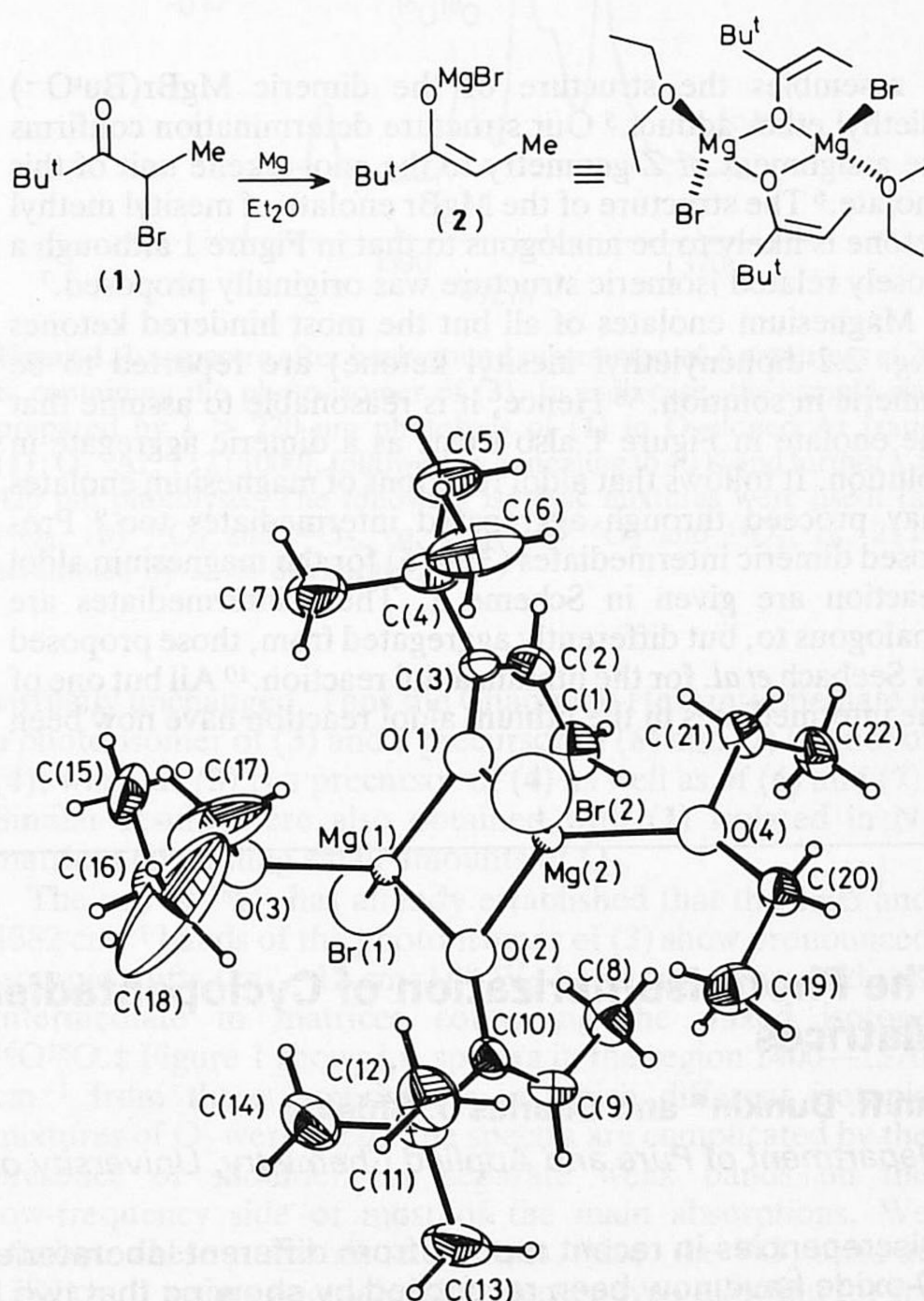


**Figure 1.** Structure of the bromomagnesium enolate of t-butyl ethyl ketone. Selected bond distances and angles: C(1)–C(2) 1.481(15), C(2)–C(3) 1.346(14), C(3)–O(1) 1.404(12), C(3)–C(4) 1.522(14), O(1)–Mg(1) 1.951(7), O(1)–Mg(2) 1.955(7), Mg(1)–Br(1) 2.417(4), Mg(1)–O(3) 2.049(9) Å; Mg(1)–O(1)–Mg(2) 95.1(3), Mg(1)–O(2)–Mg(2) 94.8(3), O(1)–Mg(1)–O(2) 84.7(3), O(1)–Mg(2)–O(2) 84.8(3), O(3)–Mg(1)–Br(1) 105.4(3)°. All other bond distances and angles are within the normally expected ranges.